Available online at www.sciencedirect.com
SCIENCE DIRECT
Journal of Photochemistry and Photobiology A: Chemistry 181 (2006) 226–232
Journal of Photochemistry and Photobiology A:Chemistry
www.elsevier.com/locate/jphotochem

# Solid-state dye-sensitized solar cell: Improved performance and stability using a plasticized polymer electrolyte

Viviane C. Nogueira, Claudia Longo, Ana Flávia Nogueira, Mauro A. Soto-Oviedo, Marco-A. De Paoli *

*Laboratório de Polímeros Condutores e Reciclagem, Instituto de Química, UNICAMP. C. Postal 6154, 13084-971 Campinas, SP, Brazil*

Received 14 September 2005; received in revised form 29 November 2005; accepted 30 November 2005
Available online 6 January 2006

**Abstract**

The addition of the plasticizer poly(ethylene glycol)methyl ether to the polymer electrolyte based on poly(epichlorohydrin-co-ethylene oxide), NaI and $I_2$ increased the ionic conductivity by one order of magnitude ($1.7 \times 10^{-4}$ S cm$^{-1}$) without compromising its electrochemical, thermal and dimensional stabilities. The plasticized polymer electrolyte presented an estimated diffusion coefficient of $2 \times 10^{-6}$ cm$^{-2}$ s$^{-1}$, ca. five times higher than the diffusion coefficient estimated for the polymer electrolyte without plasticizer. Solid-state dye-sensitized $TiO_2$ solar cells (1 cm$^2$) were assembled with the plasticized polymer electrolyte and presented an open circuit potential of 0.64 V, short-circuit current of 0.60 mA cm$^{-2}$ and an energy conversion efficiency of 1.75% under light intensity of 10 mW cm$^{-2}$. This efficiency remained unchanged for 30 days, showing that cell efficiency and stability can be improved using a plasticized polymer electrolyte.


*Keywords:* Polymer electrolyte; Ionic conductivity; Plasticizer; Solid-state dye-sensitized $TiO_2$ solar cell; Stability

## 1. Introduction

Dye-sensitized $TiO_2$ solar cells (DSSC) have been intensively investigated as potential alternatives to photovoltaic devices due to the low energy consumption for their production, low cost of raw materials and high integrated efficiency of solar energy conversion (∼10%) [1,2]. The working principle of these cells is based on electron injection from a photoexcited sensitizer dye into the conduction band of the nanocrystalline $TiO_2$ semiconductor. The original state of the dye is subsequently restored by electron donation from the electrolyte, usually an organic solvent containing a redox couple, such as iodide/triiodide. Regeneration of iodide ions is achieved at the counter-electrode by electrons from the external circuit [1,2]. The use of a liquid electrolyte still remains a critical issue in view of the practical applications of DSSC. The liquid electrolyte demands a perfect sealing of the devices in order to avoid leakage and evaporation of the solvent, which might result in low long-term stability and performance [3]. Many efforts have been made to overcome this drawback, replacing the liquid electrolytes by room temperature ionic liquids [4,5], organic and inorganic hole-transport materials [6–8], gel [9,10] and polymer electrolytes [2,11,12].

Polymer electrolytes are composed by alkaline salts (e.g. lithium or sodium salts) dissolved in a high molecular weight polymer host such as poly(ethylene oxide) (PEO) or poly(propylene oxide) (PPO) [2]. In general, DSSC assembled with polymer electrolytes exhibit lower efficiency than cells employing liquid electrolytes due to the lower ionic mobility of the $I^-/I_3^-$ species in the polymeric medium, which affects the kinetics of all the transfer processes involved in cell operation. However, in spite of the lower performance, the benefits obtained by replacement of liquid electrolytes can be worthwhile in achieving cells with improved stability [13].

Since 1996, our group has been working on DSSC using a polymer electrolyte based on poly(epichlorohydrin-*co*-ethylene oxide), P(EPI-EO), and the first results were published in 1999 [14]. The best energy conversion efficiency that we have obtained for a solid-state DSSC (active area of 1 cm$^2$) was 2.6% under 10 mW cm$^{-2}$ [11]. However, our results indicate that we have already reached the limit of the cells efficiency for a system based only on polymer and salt. Other components must be added to the system in order to ensure cells with a

* Corresponding author. Tel.: +55 19 3788 3075; fax: +55 19 3788 3023/3022.
*E-mail address:* mdepaoli@iqm.unicamp.br (Marco-A.D. Paoli).

1010-6030/$ – see front matter © 2005 Elsevier B.V. All rights reserved.
doi:10.1016/j.jphotochem.2005.11.028

better performance and to improve ionic conductivity and as a consequence $I_3^-/I^-$ mobility.

Recently, Kim et al. reported on the performance of a solid-state DSSC employing a polymer electrolyte based on poly(butyl acrylate) (PBA), NaI and $I_2$ [12]. In this study, the polymer electrolyte presented an ionic conductivity in the range of $10^{-7}$ to $10^{-6}$ S cm$^{-1}$ at room temperature, and the DSSC (active area of 0.125 cm$^2$) showed an energy conversion efficiency of 1.66% under 10 mW cm$^{-2}$. Falaras and co-workers reported a highly efficient DSSC using a composite of poly(ethylene oxide)/$TiO_2$ and LiI/$I_2$ as polymer electrolyte [15,16]. In this study, $TiO_2$ nanoparticles were introduced in the polymer electrolyte as fillers, decreasing PEO crystallinity and, as a consequence, increasing the ionic conductivity ($\sim 10^{-5}$ S cm$^{-1}$). The DSSC (active area of 0.25 cm$^2$) presented an energy conversion efficiency of 4.2% under 65 mW cm$^{-2}$.

Other efforts have tried to improve the ionic conductivity of polymer electrolytes, and one of the most successful approaches to improve this ionic conductivity consists in the addition of plasticizers (up to 50 wt.%) without compromising the thermal, electrochemical and dimensional stability. The most employed plasticizers are low molecular weight organic solvents such as propylene carbonate (PC) and ethylene carbonate (EC), or low molecular weight polymers such as poly(ethylene glycol) derivatives. The function of the plasticizer is to decrease polymer–polymer chain interactions, leading to a polymeric matrix with a low glass transition temperature ($T_g$) and a low degree of crystallinity. The presence of a plasticizer also introduces a new path for salt dissociation [17–21]. For example, Haque et al. reported on the performance and stability of a flexible solid-state DSSC based upon dye-sensitized nanocrystalline $Al_2O_3$ coated $TiO_2$ films and a plasticized polymer electrolyte of P(EPI-EO), EC, PC, NaI and $I_2$. Such devices showed an energy conversion efficiency of $\sim$5.3% under 10 mW cm$^{-2}$ [22], and this result encouraged the research of other plasticizers for these systems.

In addition, the plasticized polymer electrolyte differs considerably from gel electrolytes commonly used in DSSC. In this case, the ionic transport resembles that of a liquid system and the polymer serves primarily as a support for the conducting matrix [17–21].

In the other hand, the stability of a device is also a crucial issue considering its commercial application but there is a lack of information in the literature concerning the stability of DSSC assembled with polymer electrolytes. In this present work, we focused our efforts on the plasticizer effect of poly(ethylene glycol)methyl ether with respect to the ionic conductivity, electrochemical and thermal properties of a polymer electrolyte based on P(EPI-EO), NaI and $I_2$ and its application in solid-state dye-sensitized $TiO_2$ solar cells. We also investigated the role of the plasticizer on DSSC performance and stability.

## 2. Experimental

### 2.1. Ionic conductivity

Samples of poly(epichlorohydrin-*co*-ethylene oxide), P(EPI-EO), with a co-monomer ratio of 16/84, respectively, were used as received from Daiso Co. Ltd. (Osaka). The copolymer molecular weight reported by the supplier is $1.3 \times 10^6$ g mol$^{-1}$. The plasticizer poly(ethylene glycol)methyl ether, P(EGME), $M_w \sim 350$ (Acros) was used as received and it was chosen due to the similarity of its chemical structure and that of the copolymer matrix.

Samples of the P(EPI-EO) and P(EPI-EO)/P(EGME) system with different salt concentrations were prepared by dissolution of the copolymer, plasticizer, NaI and $I_2$ in acetone (molar ratio of $[I_3^-]/[I^-] = 10$). The P(EPI-EO)/P(EGME) systems were prepared mixing 50 wt.% of P(EPI-EO) and 50 wt.% of P(EGME). The addition of more than 40 wt.% of P(EGME) produces a polymer electrolyte with high values of ionic conductivity without loosing its dimensional stability. After dissolution with magnetic stirring for 24 h, the solutions were dropped onto a Teflon disk and evaporated under solvent saturated atmosphere conditions. The films were detached from the Teflon disks after cooling in liquid nitrogen and dried under vacuum for 144 h.

The ionic conductivity values were calculated from Nyquist plots obtained by electrochemical impedance spectroscopy (EIS). Measurements were performed with polymer electrolyte films pressed between two mirror-polished stainless steel blocking electrodes in a Mbraun dry box ($[H_2O] < 0.0001$%, under argon atmosphere), using a Eco Chimie-Autolab PGSTAT 12 potentiostat with a FRA module. The frequency range analyzed was 10 to $10^6$ Hz with amplitudes of $\pm 10$ mV over the open circuit potential ($V_{OC}$).

### 2.2. Electrochemical characterization

The electrochemical properties of the polymer electrolyte that exhibited highest ionic conductivity was investigated using a symmetric thin-layer cell, where a polymer electrolyte film was placed between two Pt coated glass-$SnO_2$:F (glass-FTO, Hartford glass, $R_s \leq 10\,\Omega$ cm$^{-2}$) electrodes with an active area of 1 cm$^2$. The film thickness (ca. 40 μm) was controlled using an adhesive tape. Cyclic voltammetry measurements were performed using a two-electrode configuration cell and the Eco Chimie-Autolab PGSTAT 10 potentiostat in the potential range of $-0.4$ to $+0.4$ V up to $-1.4$ to $+1.4$ V (versus Pt), at a scanning rate of 10 mV s$^{-1}$. The EIS measurements were performed using the Eco Chimie-Autolab PGSTAT 12 potentiostat with FRA module, over the frequency range from $10^{-2}$ to $10^6$ Hz with amplitudes of $\pm 10$ mV over the $V_{OC}$, and the results were analyzed using Boukamp software [23].

### 2.3. Thermal analysis

The thermal properties of the polymer electrolytes with different salt concentrations, prepared as described in Section 2.1, were characterized by differential scanning calorimetry (DSC) and thermogravimetric analysis (TGA). DSC curves were measured using a TA Instruments Thermal Analyser model 2100, coupled to a TA 2100 Data Analysis System, under nitrogen flow of 100 mL min$^{-1}$ and according to the following procedure: (1) heating from room temperature to 250 °C at 20 °C min$^{-1}$; (2) isothermal for 5 min at 250 °C; (3) cooling to $-100$ °C at

10 °C min$^{-1}$; (4) isothermal for 5 min at −100 °C and (5) second heating to 250 °C at a heating rate of 10 °C min$^{-1}$. TGA curves were measured using a Thermogravimetric Analyser model 2950 from TA Instruments. All measurements were done under a continuous argon flow of 100 mL min$^{-1}$, heating from room temperature to 600 °C at a heating rate of 10 °C min$^{-1}$. Before TGA and DSC analysis, all samples were dried under dynamic vacuum for 48 h to ensure elimination of solvent or water residues.

### 2.4. Dye-sensitized $TiO_2$ solar cells (DSSC)

DSSC were assembled using glass-FTO (Hartford glass, $R_s \leq 10\,\Omega\,cm^{-2}$) and glass-ITO (Delta Technologies, $R_s \leq 30\,\Omega\,cm^{-2}$) electrodes as substrates for photoelectrode and counter-electrode, respectively. Counter-electrodes (CE) were prepared by sputter depositing a thin Pt film (400 Å) onto glass-ITO electrodes. For preparation of photoelectrodes (active area of 1 cm$^2$), a small aliquot of $TiO_2$ sol–gel suspension [24] was spread using a glass rod onto the glass-FTO electrodes with an adhesive tape as spacer. The electrodes were heated at 450 °C for 30 min, cooled to ∼80 °C in a desiccator, immersed in a $1.5 \times 10^{-4}$ mol L$^{-1}$ solution of the sensitizer dye *cis*-bis(isothiocyanato)bis(2,2′-bipyridyl-4,4′-dicarboxylato)-ruthenium(II), Ruthenium-535, Solaronix) in absolute ethanol for 16 h. After that, the electrodes were rinsed with ethanol and dried. A film of the polymer electrolyte was cast onto the sensitized electrodes under a saturated solvent atmosphere. An alternative procedure for the deposition of the polymer electrolyte solutions onto sensitized electrodes consisted in casting the solution onto the electrodes placed on a hot plate at 60 °C.

The final assembly of the DSSC was done by pressing the CE against the sensitized electrode coated with the polymer electrolyte. An adhesive tape (ca. 40 μm) was placed between the two electrodes, in order to control electrolyte film thickness and to avoid short-circuiting of the cell, and the device was placed in a desiccator with $P_2O_5$ for 2 h to remove moisture.

The DSSC devices were characterized on an optical bench consisting of an Oriel Xe (Hg) 250 W lamp. Water and cut-off filters were used to avoid IR and UV radiation. The light intensity was measured with a Newport Optical Power Meter. Current–potential curves (*I–V* curves) were obtained using linear sweep voltammetry at 1 mV s$^{-1}$ using the Eco Chimie-Autolab PGSTAT 10 potentiostat. The stability tests were performed daily, irradiating each cell for 1 h at 100 and 10 mW cm$^{-2}$ in short-circuit conditions, for approximately 30 days.

## 3. Results and discussion

### 3.1. Ionic conductivity

The ionic conductivity can be calculated from the bulk electrolyte resistance value obtained from the complex impedance diagram. The ionic conductivities of P(EPI-EO)/NaI/$I_2$ and P(EPI-EO)/P(EGME)/NaI/$I_2$ samples (28 ± 1 °C, [$H_2O$] < 0.0001%), with different salt concentrations are shown in Fig. 1. In the P(EPI-EO)/NaI/$I_2$ system we can infer that the increase in salt concentration leads to an increase of ionic conductivity ($\sigma$) up to 11 wt.% of NaI, reaching a maximum value of $1.9 \times 10^{-5}$ S cm$^{-1}$. By increasing NaI concentration above this quantity, the conductivity shows a slow decrease due to the formation of ion pairing and crosslinking sites that hinders the segmental motion of the polymeric chains and as a consequence the ionic mobility decreases [25]. By adding P(EGME) to the polymer electrolyte, we observed a general increase in the ionic conductivity of the system for all salt concentrations, reaching a maximum value of $1.7 \times 10^{-4}$ S cm$^{-1}$ at 13 wt.% of NaI. The addition of the plasticizer to the polymer electrolyte allows dissolution of a higher amount of salt without significatively changing the conductivity of the system, which remains on the plateau of $10^{-4}$ S cm$^{-1}$. This result is an interesting feature for application in DSSC.

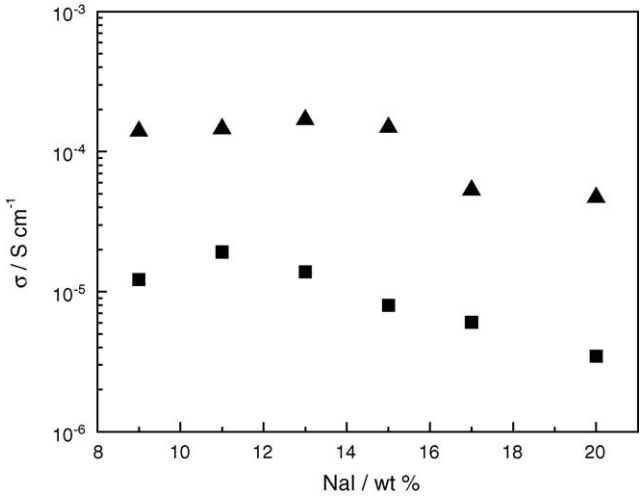


Fig. 1. Variation of the ionic conductivity of the polymer electrolytes: (■) P(EPI-EO)/NaI/$I_2$ and (▲) P(EPI-EO)/P(EGME)/NaI/$I_2$ as functions of NaI concentration (28 ± 1 °C, [$H_2O$] < 0.0001%).

In addition, it is important to emphasize that these measurements were made under a strictly controlled low-humidity atmosphere ([$H_2O$] < 0.0001%) since the presence of any residual solvent or water can considerably affect the ionic conductivity, masking the plasticizer effect [26].

### 3.2. Electrochemical characterization

The electrochemical properties of the polymer electrolytes that showed highest ionic conductivity values (P(EPI-EO) + 11 wt.% NaI + $I_2$ and P(EPI-EO)/P(EGME) + 13 wt.% NaI + $I_2$) were investigated using a symmetric thin-layer cell reproducing the conditions used in a DSSC. Cyclic voltammetry measurements revealed an electrochemical stability window of 2.4 V (versus Pt) for both polymer electrolytes, indicating that these electrolytes are suitable for application in DSSC (data not shown).

The EIS measurements carried out for the same systems are represented by the Nyquist diagrams in Fig. 2. The results revealed a decrease in the overall impedance with the addition of plasticizer. The response at high frequencies can be attributed

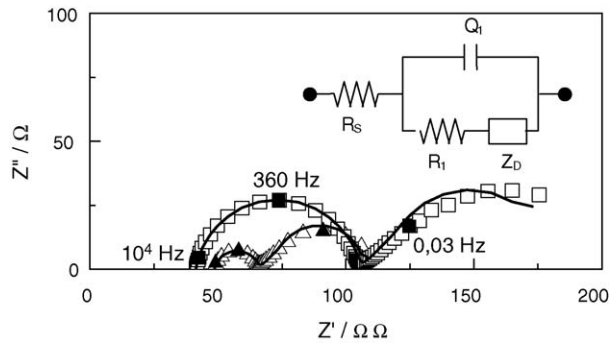


Fig. 2. Nyquist diagrams of the impedance spectra obtained for cells consisting of polymer electrolyte films placed between two Pt electrodes: (□) P(EPI-EO) + 11 wt.% NaI/$I_2$ and (△) P(EPI-EO)/P(EGME) + 13 wt.% NaI/$I_2$. Experimental data are represented by symbols while the solid lines correspond to fits obtained with Boukamp software using the equivalent circuit presented in the insert.

to the Pt|electrolyte interface, while the response at low frequencies can be associated with the diffusion process in the electrolyte [27]. An equivalent circuit (shown in Fig. 2) represented by $R_S[Q_1(R_1O_1)]$, was used to fit the EIS data using Boukamp software [23]. In this circuit, the symbol $R$ describes a resistence; $O$, intrisically related to the parameters $Y_{O_1}$ and $B$, accounts for a finite-length Warburg diffusion ($Z_D$), and $Q$ is the symbol for the constant phase element, CPE (its parameters were $Y_{O_2}$ and $n$) [27]. From the parameters obtained in the fitting using the equivalent circuit described earlier, the diffusion coefficient of the species ($D$) can be estimated from $D = l_e^2/B^2$ [28]. The diffusing length, $l_e$, can be considered as the thickness between the electrodes (thickness of the adhesive tape, 40 μm). From this, the value of $D$ can be roughly estimated.

In our case, the $D$ values increased from $4 \times 10^{-7}$ to $2 \times 10^{-6}\,cm^{-2}\,s^{-1}$ with the addition of the plasticizer. This value is very close to the diffusion coefficient for $I_3^-$ species in highly viscous solvents, such as *N*-methyl oxazolidinone ($2.8 \times 10^{-6}\,cm^2\,s^{-1}$), and in acetonitrile in a $TiO_2$ membrane ($3.4 \times 10^{-6}\,cm^2\,s^{-1}$) [29,30]. To reach equilibrium during charge transport across the cell it is necessary to have the same $D$ for the cation and the anion, and this was assumed by us in this work. In order to estimate the value of $D$ for the cation and anion separately, it would be necessary to use dc impedance, as stated in Ref. [31].

### 3.3. Thermal analysis

Table 1 exhibits the information obtained from the second heating scan of DSC curves for the samples of P(EPI-EO) and P(EPI-EO)/P(EGME) with different salt concentrations. From these curves, it was possible to obtain the glass transition ($T_g$) and melting temperatures ($T_m$), and the melting enthalpies ($\Delta H_m$). The crystallinity degree ($X_c$) of the samples was calculated from $X_c = (\Delta H_m^\circ/\Delta H_m^\circ) \times 100\%$, where $\Delta H_m$ and $\Delta H_m^\circ$ are the melting enthalpy of the sample and the melting enthalpy of 100% pure crystalline poly(ethylene oxide), respectively ($\Delta H_m^\circ = 220.81\,J\,g^{-1}$) [32]. In this study, it was not possible to calculate $T_m$, $\Delta H_m$ and $X_c$ for the copolymer in P(EPI-EO) + P(EGME) systems because it occurs in the same temperature range as the $T_m$ for P(EGME).

The increase of salt concentration contributes to a decrease in the crystallinity degree of the copolymer, as evidenced for the P(EPI-EO)/NaI/$I_2$ samples. As a consequence there is a partial conversion of the crystalline phase (formed exclusively by ethylene oxide units) into an amorphous phase after $Na^+$ complexation [33]. The addition of the plasticizer, P(EGME), shifts the polymer $T_g$ to lower temperatures, indicating that this plasticizer contributes to decrease polymer–polymer chain interactions, hence, increasing the flexibility of the polymer chains.

The thermal stabilities of the polymer electrolyte samples were determined by TGA and compared with the pure copolymer (Fig. 3(a)). For the P(EPI-EO) sample, only one mass loss step at 336 °C (maximum mass loss temperature, $T_{dec}$) is observed, associated to thermal degradation of the copolymer, due to the loss of chlorine radicals and production of HCl, in analogy to the thermal degradation of poly(vinyl chloride) [25]. The polymer electrolyte sample with 11 wt.% of NaI presented a $T_{dec}$ of 324 °C, approximately 10 °C lower than the $T_{dec}$ for the pure copolymer, indicating that the presence of salt contributes to decrease the thermal stability of the copolymer. This evidence suggests an association of the excess of $Na^+$ cations with the chlorine atoms of the epichlorohydrin repeating units. The cations weaken the C–Cl bond by removing electronic density [25,34]. The addition of P(EGME) leads to a slight decrease in the thermal stability of the copolymer ($T_{dec}$ = 298 °C). However, considering that most of the devices operate at temperatures below 120 °C, we conclude that the thermal stability is adequate for these systems.

Table 1
Data obtained from the analysis of the DSC curves for P(EPI-EO)/NaI/$I_2$ and P(EPI-EO)/P(EGME)/NaI/$I_2$ samples

| NaI/$I_2$ (wt.%) | P(EPI-EO) | | | | P(EPI-EO) + P(EGME) |
|---|---|---|---|---|---|
| | $T_m$ (±2 °C) | $T_g$ (±2 °C) | $\Delta H_m$ ($J\,g^{-1}$) | $X_c$ (%) | $T_g$ (±2 °C) |
| 0 | 28 | −53 | 26.9 | 12 | −66 |
| 9 | 36 | −51 | 19.4 | 8.8 | −58 |
| 11 | 22 | −50 | 13.2 | 6.0 | −66 |
| 13 | 21 | −51 | 9.2 | 4.2 | −61 |
| 15 | 21 | −50 | 8.2 | 3.7 | −57 |
| 17 | 23 | −49 | 7.1 | 3.2 | −67 |
| 20 | 24 | −49 | 6.4 | 2.9 | −63 |

*Note*: $T_m$ for copolymer in the P(EPI-EO) + P(EGME) system is not shown because it occurs in the same temperature range as the $T_m$ for P(EGME).

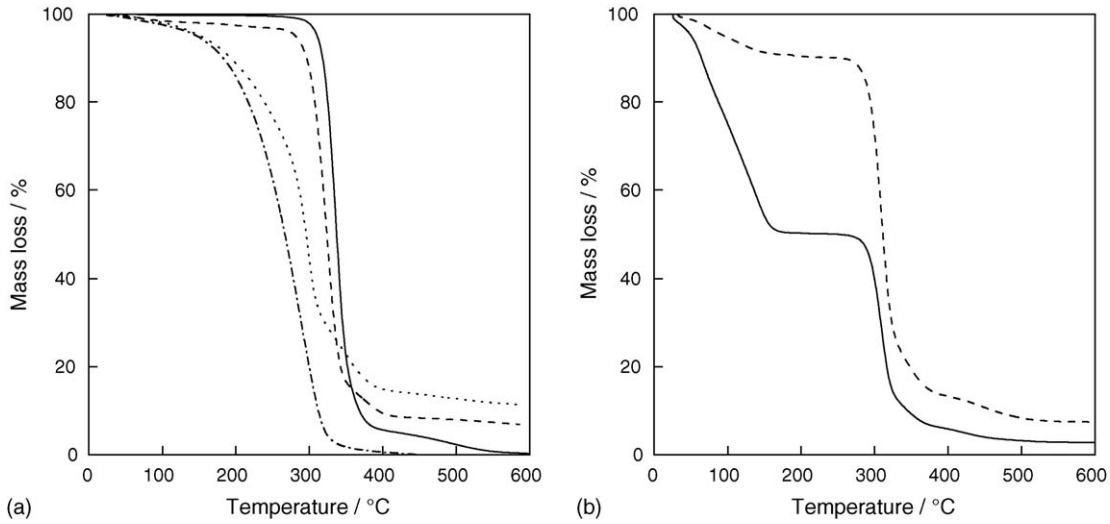


Fig. 3. (a) Thermogravimetric curves for (—) P(EPI-EO), (- - -) P(EPI-EO) + 11 wt.% NaI/$I_2$, (. . .) P(EGME) and (-·-) P(EPI-EO)/P(EGME) + 13 wt.% NaI/$I_2$ samples. (b) Thermogravimetric curves for P(EPI-EO) + 11 wt.% NaI/$I_2$ samples prepared by casting the polymer electrolyte under saturated solvent atmosphere: (—) first and (- - -) fifth day.

Fig. 3(b) shows the thermogravimetric curves obtained for polymer electrolyte samples containing P(EPI-EO) + 11 wt.% of NaI + $I_2$. These samples were prepared by casting the polymer electrolyte under a saturated solvent atmosphere, reproducing the conditions usually employed in a DSSC. Both samples were prepared the same day and thermogravimetric analyses were performed immediately after the preparation of one sample (first day) and again on the fifth day. TGA curves for both samples presented two mass loss steps. The first step was associated to the loss of residual solvent and moisture and the second one was associated to the thermal degradation of the copolymer, as discussed earlier. For the sample analyzed in the first day, 50% of mass loss is attributed to residual solvent and moisture. After 4 more days this loss was reduced to 10%. These results indicate that casting the polymer electrolyte from a solution leaves a high amount of residual solvent and moisture in the device. Thus, a new methodology was employed to avoid residual solvent.

### 3.4. Dye-sensitized $TiO_2$ solar cells (DSSC)

The current–potential curves (*I–V*) obtained under different light intensities for a DSSC assembled with a P(EPI-EO) + 11% NaI/$I_2$ polymer electrolyte are represented in Fig. 4, and open circuit potentials ($V_{OC}$) ranging from 0.60 to 0.68 V were measured. When the irradiation intensity was increased from 10 to 100 mW cm$^{-2}$, the short-circuit current ($I_{SC}$) changed from 0.38 to 2.53 mA cm$^{-2}$, and the energy conversion efficiency ($\eta$) decreased from 1.6 to 1.0%. These values are comparable to other studies and are lower than those exhibited by DSSC assembled with liquid electrolytes [11,35]. As expected, $\eta$ decreases with the increase in light intensity due to the low ionic mobility of the redox species in the polymer electrolyte retarding the kinetics of the dye regeneration reaction. Fig. 5 shows the variation of $\eta$ as a function of time for this DSSC. The data revealed that the cell performance showed a decrease of 75% in the $I_{SC}$ after 35 days ($I_{SC}$ = 0.67 mA cm$^{-2}$ under 100 mW cm$^{-2}$). A similar behaviour was obtained in a previous study involving a similar DSSC assembled with P(EPI-EO) containing 9 wt.% of NaI [36]. In this study [36], a DSSC device was irradiated daily for 12 h under 100 mW cm$^{-2}$ and 12 h under 10 mW cm$^{-2}$, for a period of 70 days. The $I_{SC}$ decreased from 2.7 to 0.7 mA cm$^{-2}$ (100 mW cm$^{-2}$) after 35 days of continuous cell irradiation.

Our stability tests corroborate the data obtained from thermogravimetric analysis, the initial drop in cell efficiency can be related to the loss of residual solvent (in our case acetone) which remains in polymer host. As the solvent evaporates, the ionic conductivity of the polymer electrolyte decreases and, as a consequence, the mobility of charge carriers. The loss of solvent results in the formation of empty holes (spaces) contributing to increased resistance and lowering the contact between the elec-

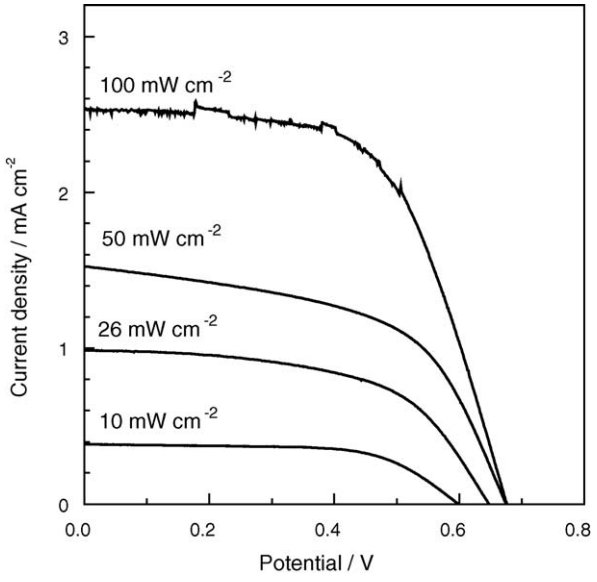


Fig. 4. Current–potential curves obtained under different light intensities for a solid-state DSSC assembled with a P(EPI-EO) + 11 wt.% NaI/$I_2$ polymer electrolyte.

Table 2
Data obtained from the *I–V* curves for the DSSC assembled with different polymer electrolytes deposited by casting at 60 °C

| Polymer electrolyte | Light intensity (mW cm$^{-2}$) | 1st day | | | 31st day | | |
|---|---|---|---|---|---|---|---|
| | | $I_{SC}$ (mA cm$^{-2}$) | $V_{OC}$ (V) | $\eta$ (%) | $I_{SC}$ (mA cm$^{-2}$) | $V_{OC}$ (V) | $\eta$ (%) |
| P(EPI-EO) + 11% NaI/$I_2$ | 100 | 0.55 | 0.75 | 0.19 | 0.49 | 0.73 | 0.17 |
| | 10 | 0.28 | 0.70 | 0.88 | 0.25 | 0.67 | 0.69 |
| P(EPI-EO) + P(EGME) + 13% NaI/$I_2$ | 100 | 1.88 | 0.70 | 0.52 | 1.46 | 0.70 | 0.44 |
| | 10 | 0.60 | 0.64 | 1.75 | 0.61 | 0.67 | 1.76 |

trodes. The presence of residual solvent after DSSC assembly was also reported by Kim et al. [12]. In this work [12], a solid-state DSSC employing poly(butyl acrylate) (PBA), NaI and $I_2$, as polymer electrolyte, presented an energy conversion efficiency of 4% (10 mW cm$^{-2}$) on the first day. However, $\eta$ dropped to 1.66% after vacuum drying for 1 day, indicating the presence of residual solvent after the device assembly.

Based on these results, we employed an alternative procedure for the DSSC assembly. In this case, the deposition of polymer electrolyte solution consisted of casting the solution onto the $TiO_2$/dye photoelectrode placed on a hot plate at 60 °C. Haque et al. previously demonstrated that this simple procedure results in a high degree of penetration of the polymer electrolyte into the $TiO_2$ film pores [22]. Since the plasticizer has a high boiling point, it is not removed by this procedure. In addition, by removing the residual acetone the empty spaces left behind are readily replaced by the plasticizer. Table 2 summarizes the results obtained from the *I–V* curves for DSSC assembled with different polymer electrolytes using this new procedure. A significant increase in performance of the DSSC is observed for the DSSC assembled with the plasticized polymer electrolyte. The evolution of $\eta$ with time for both cells is represented in Fig. 6 and shows that the performance of both cells remained constant for 31 days. These results indicate that the removal of acetone by heating contributes to improving the stability of the DSSC.

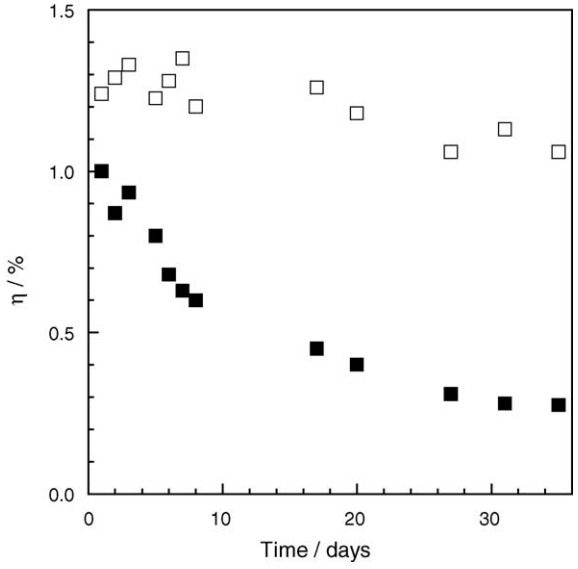


Fig. 5. Variation of energy conversion efficiency as a function of time for a solid-sate dye-sensitized $TiO_2$ solar cell assembled with a P(EPI-EO) + 11 wt.% NaI/$I_2$ polymer electrolyte, under (□) 10 and (■) 100 mW cm$^{-2}$.

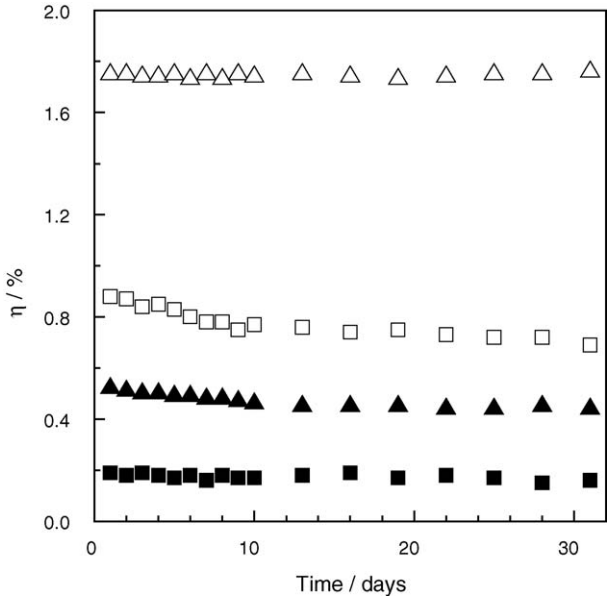


Fig. 6. Variation of energy conversion efficiency as a function of time for a solid-state DSSC assembled with different polymer electrolytes deposited by casting at 60 °C: (■, □) P(EPI-EO) + 11 wt.% NaI/$I_2$ and (▲, △) P(EPI-EO)/P(EGME) + 13 wt.% NaI/$I_2$, under 10 mW cm$^{-2}$ (open symbols) and 100 mW cm$^{-2}$ (solid symbols).

## 4. Conclusion

The addition of poly(ethylene glycol)methyl ether to the polymer electrolyte based on poly(epychlorydrin-*co*-ethylene oxide), NaI and $I_2$ contributed to increase the ionic conductivity by one order of magnitude. The addition of the plasticizer did not compromise the electrochemical, thermal and dimensional stabilities of the polymer electrolyte. Our results indicate that using a plasticized polymer electrolyte with some modification in cell preparation are crucial for designing solid-state dye-sensitized $TiO_2$ solar cells with improved performance and stability.

## Acknowledgements

The authors thank Fapesp (Proc. no. 03/05204-1), CNPq and Capes for financial support, Daiso Co. Ltd., Osaka, for supplying the polymer samples and Prof. Carol H. Collins who has corrected this manuscript.

## References


[1] B. O'Reagan, M. Grätzel, Nature 353 (1991) 737–740.
[2] A.F. Nogueira, C. Longo, M.-A. De Paoli, Coord. Chem. Rev. 248 (2004) 1455–1468.
[3] M. Grätzel, J. Photochem. Photobiol. A: Chem. 164 (2004) 3–14.
[4] P. Wang, S.M. Zakeeruddin, J.-E. Moser, R.H. Baker, M. Grätzel, J. Am. Chem. Soc. 126 (2004) 7164–7165.
[5] H. Matsumoto, T. Matsuda, T. Tsuda, R. Hagiwara, Y. Ito, Y. Miyazaki, Chem. Lett. 1 (2001) 26–27.
[6] Q.B. Meng, K. Takahashi, X.-T. Zhang, I. Sutanto, T.N. Rao, O. Sato, A. Fujishima, H. Watanabe, T. Nakamori, M. Uragami, Langmuir 19 (2003) 3572–3574.
[7] D. Gebeyehu, C.J. Brabec, N.S. Sariciftci, D. Vangeneugden, R. Kiebooms, D. Vanderzande, F. Kienberger, H. Schindler, Synth. Met. 125 (2002) 279–287.
[8] J. Bandara, H. Weerasinghe, Sol. Energy Mater. Sol. Cells 85 (2005) 385–390.
[9] J. Kang, W. Li, X. Wang, Y. Lin, X. Li, X. Xiao, S. Fang, J. Appl. Electrochem. 34 (2004) 301–304.
[10] W. Kubo, K. Murakoshi, T. Kitamura, S. Yoshida, M. Hakuri, K. Hanabusa, H. Shirai, Y. Wada, S. Yanagida, J. Phys. Chem. B 105 (2001) 12809–12815.
[11] A.F. Nogueira, J.R. Durrant, M.-A. De Paoli, Adv. Mater. 13 (2001) 826–830.
[12] J.H. Kim, M.-S. Kang, Y.J. Kim, J. Won, Y.S. Kang, Solid State Ionics 176 (2005) 579–584.
[13] C. Longo, M.-A. De Paoli, J. Braz. Chem. Soc. 14 (2003) 889–901.
[14] A.F. Nogueira, N. Alonso-Vante, M.-A. De Paoli, Synth. Met. 105 (1999) 23–27.
[15] G. Katsaros, T. Stergiopoulos, I.M. Arabatzis, K.G. Papadokostaki, P. Falaras, J. Photochem. Photobiol. A: Chem. 149 (2002) 191–198.
[16] T. Stergiopoulos, I.M. Arabatzis, G. Katsaros, P. Falaras, Nanoletters 2 (2002) 1259–1261.
[17] J. Kang, W. Li, X. Wang, Y. Lin, X. Xiao, S. Fang, Electrochim. Acta 48 (2003) 2487–2491.
[18] M. Kumar, S.S. Sekhon, Eur. Polym. J. 38 (2002) 1297–1304.
[19] M.M. Silva, S.C. Barros, M.J. Smith, J.R. MacCallum, J. Power Sources 111 (2002) 52–57.
[20] F.M. Gray, Solid Polymer Electrolyte: Fundamentals and Technological Applications, Verlag Chemie, New York, 1991, 108–111.
[21] F.M. Gray, M. Armand, in: T. Osaka, M. Datta (Eds.), New Trends in Electrochemical Technology: Energy Storage Systems for Electronics, Gordon and Breach Science Publishers, New York, 2000, pp. 351–406.
[22] S.A. Haque, E. Palomares, H.M. Upadhyaya, L. Otley, R.J. Potter, A.B. Holmes, J.R. Durrant, Chem. Commun. 24 (2003) 3008–3009.
[23] B.A. Boukamp, EQUIVCRT Version 4.51, University of Twente, The Netherlands, 1995.
[24] C.-C. Wang, J.Y. Ying, Chem. Mater. 11 (1999) 3113–3120.
[25] G.G. Silva, N.H.T. Lemes, C.N. Polo da Fonseca, M.-A. De Paoli, Solid State Ionics 93 (1997) 105–116.
[26] A.E. Wolfenson, R.M. Torresi, T.J. Bonagamba, M.-A. De Paoli, H. Panepucci, J. Phys. Chem. B 101 (1997) 3469–3473.
[27] C. Longo, A.F. Nogueira, M.-A. De Paoli, J. Phys. Chem. B 106 (2002) 5925–5930.
[28] J.R. Macdonald, Impedance Spectroscopy: Emphasizing Solid Materials and Systems, John Wiley, New York, 1987.
[29] N. Papageorgiou, M. Grätzel, P.P. Infelta, Sol. Energy Mater. Sol. Cells 44 (1996) 405–438.
[30] Z. Zebede, S.E. Lindquist, Sol. Energy Mater. Sol. Cells 51 (1998) 291–303.
[31] Y.-T. Kim, E.S. Smotkin, Solid State Ionics 149 (2002) 29–37.
[32] A. Kaminska, H. Kaczmarek, J. Kowalonek, Polymer 40 (1999) 5781–5791.
[33] A.F. Nogueira, M.A.S. Spinacé, W.A. Gazotti, E.M. Girotto, M.-A. De Paoli, Solid State Ionics 140 (2001) 327–335.
[34] L. Costa, A.M. Gad, G. Camino, G.G. Cameron, M.Y. Qureshi, Macromolecules 25 (1992) 5512–5518.
[35] M.K. Nazeeruddin, A. Kay, I. Rodicio, R. Humphry-Baker, E. Muller, P. Liska, N. Vlachopoulos, M. Grätzel, J. Am. Chem. Soc. 115 (1993) 6382–6390.
[36] A.F. Nogueira, Grätzel solar cells with polymer electrolyte, PhD Thesis, Universidade Estadual de Campinas, Campinas, 2001.